Improving some physicochemical characteristics of environmentally friendly insulating liquids for enhanced sustainability in subpolar transformer applications

S.O. Oparanti [a], I. Fofana [a,*], R. Zarrougui [c], R. Jafari [b], K.M.L. Yapi [a]

[a] Canada Research Chair tier 1 on the Aging of Power Network Infrastructure (ViAHT) University of Quebec at Chicoutimi, Chicoutimi, QC G7H 2B1, Canada
[b] International Research Center on Atmospheric Icing and Power Engineering (CENGIVRE). Department of Applied Sciences, University of Quebec at Chicoutimi (UQAC), 555, boul. de l'Université, Chicoutimi, Québec G7H 2B1, Canada
[c] Department of Basic Sciences, University of Quebec at Chicoutimi (UQAC), 555, boul. de l'Université, Chicoutimi, Québec G7H 2B1, Canada

ARTICLE INFO

ABSTRACT

Mineral-based insulating liquids have been crucial in the power sector as coolants and insulators for several years. However, environmental concerns surrounding these liquids have prompted a search for alternatives. Plant-based liquids are now emerging as promising options for transformer insulation due to their eco-friendly nature and minimal contribution to exacerbating global warming. Yet, some properties of plant-based insulating liquids lag behind mineral oil, notably in viscosity, oxidation stability, and pour point. This study explores a blend of canola oil and methyl ester from palm kernel oil to achieve an oil blend with reduced viscosity and improved oxidation stability. ASTM D 2440 guided the selection process through oxidative investigative analyses, considering factors like acidity, viscosity, FTIR, and dielectric spectroscopy. The sample combining equal parts canola oil and methyl ester exhibited superior oxidation stability. Moreover, to enhance the chosen blend's crystallization temperature, Taguchi-Grey relational analysis was used with Viscoplex 10–312 and Viscoplex 10–171 pour point depressants. The optimal performance, derived from Grey relational grading, was achieved when 0.7 wt% of both depressants was added to the base liquid. This synthesized liquid, comprising 50% canola oil, 50% methyl ester from palm kernel oil, and 0.7 wt% of both depressants, presents itself as a more effective green alternative insulating liquid in the industry, reducing the environmental impact caused by mineral oil.

1. Introduction

Stringent environmental regulations on fossil-based energy sources have propelled the emergence of green-insulating liquids as viable substitutes for mineral-based insulating oils [1]. Although mineral oils have excellent insulating and cooling properties, their leakage or spills from transformers pose significant threats to the environment, causing pollution and endangering aquatic life. Additionally, in the event of an explosion, mineral oil releases greenhouse gases, aggravating climate change and global warming. Moreover, mineral oil's limited biodegradability, non-renewable nature, and inadequate fire resistance further accentuate its environmental limitations [2]. Predominantly derived from plants, particularly plant seeds, green insulating liquids offer significant advantages, including biodegradability, eco-friendliness, low flammability, and minimal volatility [1]. In recent times a considerable number of transformers have been operating on natural esters due to their excellent insulating properties and eco-friendliness. [3,4]. Among the plants where these green liquids are obtained are rapeseed, soybeans, and canola. The extracted seed oils often vary between saturated and unsaturated fatty acids in their chemical structures. However, natural esters have notable drawbacks. Among the shortfalls of natural esters are high viscosity, high pour point, and poor stability in terms of oxidation [2,5–8]. These limitations are largely due to the natural ester fatty acid chemical structure [9]. Oils rich in unsaturated fatty acids are susceptible to oxidation, yet they exhibit favorable cold flow characteristics owing to the presence of long-chain fatty acids that impede oil crystallization. Conversely, oils containing saturated fatty acids display contrasting attributes to those of unsaturated fatty acids. [10,11].

The deterioration of vegetable-based oils primarily results from

oxidation and or hydrolysis, potentially leading to a swift decline in the insulating effectiveness of the liquid. [12]. The oxidation mechanism within natural esters is illustrated in the reaction scheme depicted in Fig. 1, while the hydrolysis reaction process of natural esters is detailed in reference [11]. The initial reaction stage (I) is referred to as the initiation stage. During this phase, an initiator, such as heat, light, or radiation, prompts the splitting of hydrocarbon molecules into hydrocarbon radicals (R*) and hydrogen (H) [13]. During the propagation stage (II), a reaction takes place between the free radicals and oxygen, resulting in the generation of peroxides. Subsequently, the interaction between the free peroxide radicals and hydrocarbon molecules produces hydroperoxides, which contribute to the degradation of the insulating system's quality. It is crucial to highlight that following the propagation stage, two distinct possibilities emerge: the termination stage (III) and the autocatalytic stage (IV). During the termination stage, available radicals engage in reactions, resulting in the creation of stable oxidation products [14]. Conversely, in the autooxidation stage, the primary oxidation product, hydroperoxide, undergoes decomposition and the products react with the hydrocarbon molecules to form alcohol and water molecules. The radicals generated by the autocatalytic reaction sustain the ongoing reaction over time [13]. Properties of insulating liquids that change at the autooxidation and termination stages include color, acidity, and moisture content. Several antioxidants have been employed in the literature for enhancing the oxidation stability of insulating liquids [15] and the equation of reaction between the radicals and the antioxidants can be seen in [14].

The crystallization temperature also poses a significant challenge to the practical utilization of natural esters in sub-zero conditions. Mitigating this concern involves incorporating pour point depressants, also referred to as anti-crystallizing agents. These agents effectively lower the pour point temperature of insulating liquids, impeding their propensity to crystallize with ease under subzero temperatures. In reference [2], an optimization study of various pour point depressants was performed, and the results indicated that polymethacrylate demonstrated exceptional performance. Among the tested depressants, polymethacrylate showed the most favorable and effective results in lowering the pour point of the vegetable oil, significantly improving its cold flow properties. Figs. 2a and 2b display three-dimensional representations of oil samples, illustrating one sample without the depressant and the other with its inclusion. It is crucial to note that introducing the depressant into the base liquid does not alter the oil's molecular characteristics. Rather, its function lies in impeding the straightforward crystallization of the base liquid, leading to a notable enhancement in the liquid's overall flow attributes.

As previously mentioned, the cold flow behavior and oxidation stability of vegetable-based insulating liquids are directly impacted by the fatty acid composition, specifically the balance of saturated and unsaturated fatty acids. Therefore, having a vegetable-insulating liquid that exhibits both good cold flow properties and oxidation stability is crucial. Table 1 provides a comparison of various vegetable oils and their fatty acid compositions. Canola oil stands out due to its high percentage of
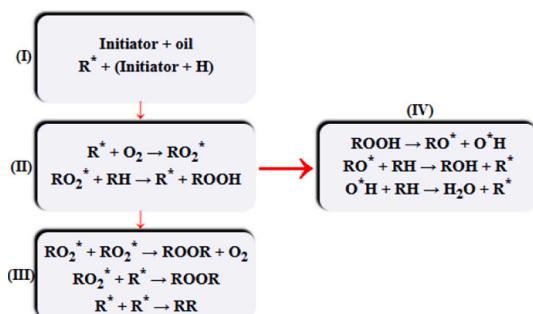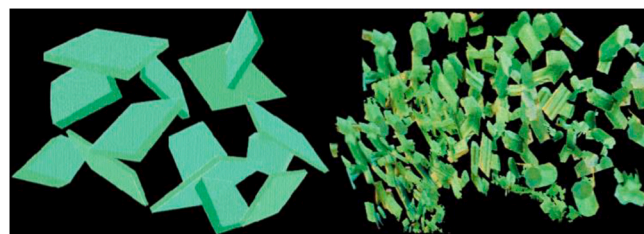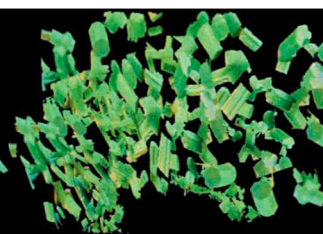

a: Oil without depressant   b: Oil with depressant

Fig. 2a. Oil without depressant.

monounsaturated fatty acids. This composition places canola oil within the range of oils with excellent oxidation stability and a relatively low pour point temperature. The experimental investigation on the potential of several insulating oils done in [16] shows that canola oil has an outstanding performance relative to other oils. Canola seed originates from Canada and it is a derivative from rapeseed cultivars of *Brassica napus* and *Brassica rapa* [17]. The seed is usually planted in the spring and takes 3 to 4 months before the harvest [18]. In recent times, canola oil seed has been ranked the third most important oilseed in the world after Soybeans and Palm, and the third source of oil around the globe [19]. The abundance of canola oil cannot be overemphasized, and it is currently finding several applications in high-voltage engineering due to its properties [1]. Also, palm kernel oil is known for its relatively high percentage of saturated fatty acids, which contributes to its stability against oxidation [6,20,21]. Palm kernel oil holds significant importance in the world as one of the topmost essential vegetable oils [22]. Due to its stable nature, palm kernel oil is widely utilized in the food industry, cosmetic industry, and as a raw material for biofuel production [23–25].

The design of experiment using the Taguchi method is a commendable approach for parameter optimization. This technique effectively minimizes costs while yielding optimal combinations of processing parameters [26,27]. Furthermore, grey relational analysis finds application in engineering for the optimization of multiple performance attributes and the assessment of process parameters. The term "grey" symbolizes incompleteness and finds its roots in the notion of a "grey box," which denotes a partially structured entity situated between a black box and a white box [28]. When a factor exists between two clearly defined extreme parameters, it is referred to as a grey parameter. Numerous instances of this method's application are evident in the literature [29–32]. The distinctiveness of this approach resides in its capacity to assess both quantitative and qualitative relationships among processing parameters, particularly when confronted with incomplete or uncertain information [33].

This study investigates the properties of mixed oil; canola oil and methyl ester from palm kernel oil. The aim is to achieve a liquid with low viscosity, good oxidation stability, and good cold flow properties. The two oils were mixed in different percentage ratios and a desired base oil was selected. The selection of the base liquid was based on evaluating its oxidation stability. Following the selection of the base liquid, the study proceeds to optimize two distinct pour point depressants on the chosen base liquid using the Taguchi Grey relational analysis. The investigation into improving natural insulating liquids holds great significance within the industry. This research aids in the swift adoption of natural esters, facilitating their substitution for mineral oil and reducing environmental concerns.

2. Experimental

2.1. Materials and chemicals

In this work, commercially available canola oil and crude palm kernel oil were utilized. The materials used, including methanol
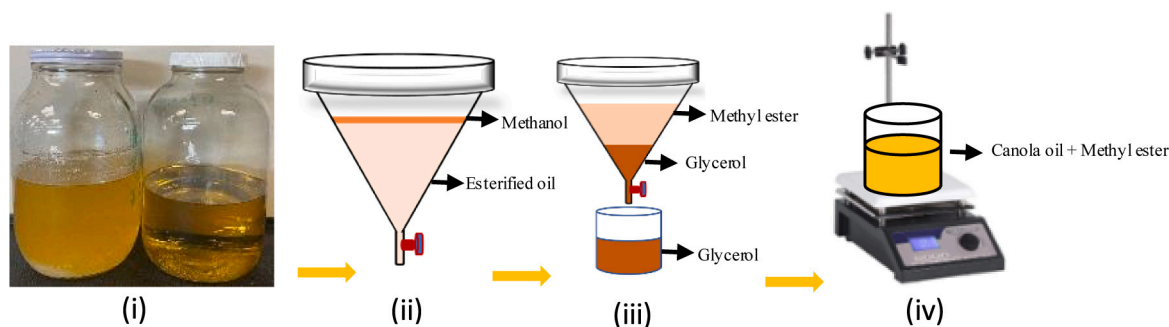

Fig. 1. Oxidation reaction scheme of natural ester insulating liquid.

Fig. 2b. Oil with depressant.

Table 1
Fatty acid percentage composition of some selected vegetable oils.

Fatty acid	Palm Kernel oil[b]	Groundnut oil[b]	Jatropha curcas oil[b]	Sunflower oil[b]	Canola oil[a]	Neem oil[c]
Oleic (18:1)	15.4	58.68	44.7	21.1	61.8	44.5
Linoleic (18:2)	2.4	21.77	32.8	66.2	19.1	18.3
Palmitic (16:0)	8.4	8.23	14.2	–	4	18.1
Stearic (18:0)	2.4	2.46	7.0	4.5	2	18.1
Lauric (12:0)	47.8	0.28	–	–	–	–
Saturated	82.1	16.81	21.6	11.3	7.4	37
Monounsaturated	15.4	58.79	45.4	21.1	63.3	44.5
Polyunsaturated	2.4	22.11	33	66.2	28.1	18.5

[a] Agenbag [34]; [b]Aransiola et al. [35]; [c]Martins et al. [36].

(99.8%), isopropyl alcohol (99.8%), phenolphthalein, citric acid pellet, anhydrous NaOH pellet ($\geq$), sulfuric acid (99.9%), filter paper, and KOH pellet, were all obtained from Sigma Aldrich. Additionally, the bleaching earth, Tonsil Standard 310 FF, was sourced from the TER chemical distribution group in Germany. The anti-crystallizing agents, VISCO-PLEX 10–312 and VISCOPLEX 10–171 were obtained from Evonik Oil Additives USA, Inc. VISCOPLEX 10–312 was considered for long-chain fatty acids and VISCOPLEX 10–171 was considered for short-chain fatty acid.

2.2. Sample preparation

The canola oil used is of industrial standard quality, and it does not require any purification process. Its quality is already suitable for the intended purposes without the need for further refinement or purification. However, the palm kernel oil is received from the extraction source which needs proper purification. The oil was degummed, neutralized, and bleached following the method reported in reference [37]. The palm kernel oil was heated to 60 °C on a SH-3 magnetic stirrer coupled with heater. Citric acid solution (1.5 ml, 30% w/w) was added to 200 ml of palm kernel oil and the temperature was kept constant while stirring for 30 min. The acid neutralization was done using NaOH solution. 4 ml of NaOH solution (8% w/w) was added to the mixture of oil and citric acid. The entire solution was stirred for 30 min at a constant temperature monitored by a digital thermocouple system. The color pigment which is an indication of the presence of elements in the oil was removed using a bleaching earth, Tonsil Standard 310 FF. The bleaching earth was also used to remove any traces of prooxidant and ionic impurities from the oil [38]. All the residues were collected through Whatman number 1 filter paper. The filtered oil starts nucleating and becomes cloudy at room temperature, however, after the filtration using Whatman number 42 having a porosity of 2.5 μm, a clear and stable liquid at ambient temperature was observed, Fig. 3(i). The palm kernel oil sample was further modified to satisfy low-temperature operational requirements and to enhance its heat exchange properties by lowering its viscosity. The transesterification reaction mentioned in references [37, 39, 40] was used for this purpose. Upon purifying the oil, the concentration of free fatty acids was analyzed and observed to be higher than 1%. This value
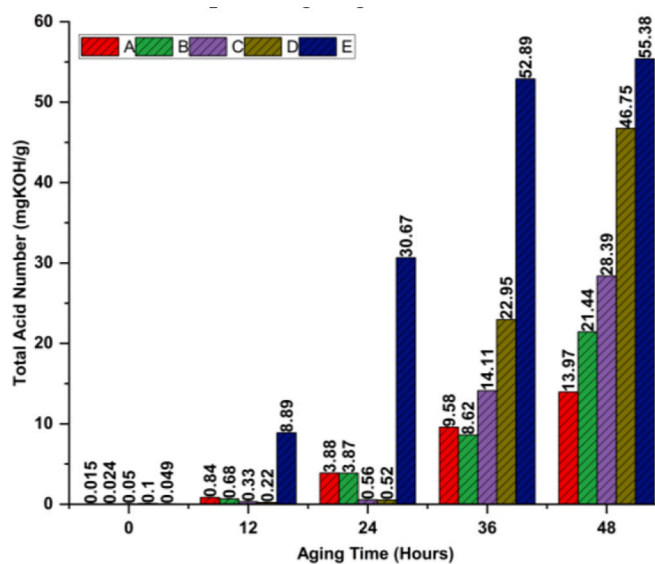

Fig. 3. Filtered oil with Whatman number 1 and number 42 filter paper respectively.

exceeds the recommended threshold for alkaline transesterification reaction, as it could hinder the separation of the ester from glycerol, leading to reduced yield and formation rate of methyl ester [41,42]. When a high percentage of free fatty acids (FFA) is present during transesterification, it can result in these FFAs reacting with the alkaline catalyst, leading to the formation of soap through saponification. This soap formation becomes problematic as it interferes with the separation of esters from glycerol, ultimately reducing the overall yield of methyl ester production. Consequently, to address this issue, acid esterification of the oil was performed using concentrated sulfuric acid and methanol. This process facilitates the transformation of the oil's free fatty acids into esters. The quantity of concentrated sulfuric acid used in the process is equal to 5% of the total free fatty acid content present in the oil sample.

Additionally, the amount of methanol utilized is equivalent to 20% of the weight of the oil. The reaction mixture was stirred for 60 min at 60 °C. After completion, the mixture was transferred to a separatory funnel, where it was allowed to form distinct layers. The undesired layer was then discarded, and the acidity of the remaining oil was measured, Fig. 3(ii). The esterified oil's free fatty acid content decreased to 0.833%. Subsequently, transesterification was carried out on the oil using NaOH as a catalyst along with methanol. The blend of oil and methoxide was stirred for 60 min at a temperature of 60 °C. The resulting mixture was then transferred to a separatory funnel to separate the glycerol from the methyl ester, Fig. 3(iii). To eliminate any traces of NaOH and dissolved soap, the mixture was washed using warm distilled water. Both the canola oil and the synthesized methyl ester were subjected to degassing and dehumidification within a vacuum oven operating at 60 °C. This process effectively decreased the moisture content of the oils to levels below 200 ppm (ppm), in accordance with the guidelines outlined in ASTM D6871 [43,44]. The preparation of the base samples was conducted in alignment with the specifications detailed in Table 2. The composite samples were mixed with a magnetic stirrer as shown in Fig. 3 (iv) for a homogenous mixture.

2.3. Oxidation stability assessment

The prepared samples were subjected to an accelerated thermo-oxidative stability test in the presence of oxygen using K121XX 6-unit oxidation stability bath according to ASTM D2440 [45]. In this process, the samples were consistently heated at a constant temperature (110 °C), while oxygen was introduced at a rate of 1 l per hour. At intervals of 12 h, samples were retrieved for examination. The analysis encompassed assessments of acidity, viscosity, Fourier Transform Infrared spectroscopy (FTIR), and dielectric spectroscopy, all contributing as pivotal factors in determining the selection of the base sample.

2.4. Acid value measurement

An increase in acidity is an important parameter that can be used for determining the stability of an insulating liquid. A titrimetric method of analysis was used to determine the total acid number of the aged oil sample. 0.1 M solution of KOH was titrated against 1 g of oil containing 20 ml of isopropyl alcohol and 2–3 drops of phenolphthalein indicator. The total acid number was calculated using Eq. 1 and the results were reported in mgKOH/g.

TAN is the total acid number, 0.1 N is the concentration of KOH, 56.1 g/mol is the molar mass of KOH, E_p is the equivalent point at which a clear color change is observed when KOH solution is titrated against the oil solution, B_v is the equivalent point of the reagent and W is the mass of the oil.

$$TAN = \frac{0.1 \times 56.1 \times (E_P - B_V)}{W} \qquad (1)$$

Table 2
Sample nomenclatures and their initial properties.

Sample	Ratio	Acid value (mgKOH/g)	Viscosity (cSt)
A	100% Canola based oil	0.015	37.96
B	75% of canola-based oil +25% methyl ester	0.024	18.75
C	50% of canola-based oil +50% methyl ester	0.05	9.60
D	25% of canola-based oil +75% methyl ester	0.1	5.68
E	100% methyl ester	0.049	3.39

2.5. Viscosity

The ASTM D445 method was employed to measure the kinematic viscosity of both fresh samples and those that had undergone aging for a duration ranging from 12 to 48 h [46]. The measurement was conducted at a temperature of 40 °C utilizing the KV3000 Series, a kinematic viscosity water bath. To guarantee consistent temperature conditions throughout the measurement procedure, an Isotemp 3016D unit was also integrated. The oil sample was allowed to flow under gravity through the capillary of the glass viscometer and the time taken for the oil to transverse the orifice was recorded. To ensure precision and consistency, the measurement was conducted in triplicate and the average was considered.

2.6. Fourier transform infrared spectroscopy (FTIR)

The changes in the chemical composition of the oil samples resulting from accelerated thermal aging were investigated using Fourier Transform Infrared Spectroscopy (FTIR). This analytical technique unveils both the distinct patterns and the specific functional groups of newly formed bonds within the insulating liquids. The analysis was conducted utilizing the PerkinElmer Spectrum One FT-IR Spectrometer, spanning the wavelength range from 450 cm^{-1} to 4000 cm^{-1}. The absorbed radiation quantity by the samples was captured by the detector and plotted against the wavenumber of the absorbed radiation. The results were used to analyze the stability of the samples when exposed to accelerated thermal aging.

2.7. Dielectric spectroscopy

The decline in the insulating characteristics of insulating liquids coincides with a rise in both the dielectric permittivity and the dielectric loss. This phenomenon occurs due to the oxidation of insulating liquids, which leads to the formation of water, acids, and other polymeric substances. These resultant byproducts can escalate the conductivity level of the liquid and degradation of transformer components which eventually exerts a detrimental influence on the longevity of transformers. To thoroughly examine and analyze the dielectric loss of the samples, the Novocontrol Alpha-A High-Performance Frequency Analyzer was employed. The cylindrical sample test cell was filled with oil samples, and the frequency spectrum was captured within the range of 10^{-2} Hz to 10^3 Hz at ambient temperature.

2.8. Low temperature properties and Taguchi experimental approach

After identifying an appropriate insulating liquid based on the outcomes of the aforementioned experimental analysis, the impact of two pour point depressants on the oil sample was investigated. The crystallization temperature, representing the point at which a liquid transforms into a crystalline state, was determined through the use of differential scanning calorimetry (DSC) with a DSC Q250 instrument (TA Instruments). A measured quantity of the sample was loaded into an aluminum crucible, sealed with a crucible sealer, and inserted into the DSC furnace. Subsequently, the sample was subjected to cooling, transitioning from −20 °C to −80 °C at a cooling rate of 5 °C per minute. Given that the liquid consists of a blend of both long-chain fatty acids and short-chain fatty acids, an optimized evaluation of the combined effects of these depressants on the base liquid was conducted using the Taguchi approach, facilitated by Minitab software. This methodology aims to unveil the optimal configuration of processing parameters. The specific experimental factors and their corresponding levels are outlined in Table 3. In this study, two factors were considered, each with two distinct levels. The design of the experiment was constructed using the L4 orthogonal array, which encompasses 4 rows – equivalent to the experimental runs. This arrangement is denoted as L4 (2**2) and is presented in Table 4. The experimental runs were duly considered in the

Table 3

Experimental factors and their corresponding levels.

Factors	Levels (wt%)	
	1	2
VISCOPLEX 10–171	0.7	1.0
VISCOPLEX 10–312	0.7	1.0

Table 4

Experimental output of the L4 orthogonal test.

Experimental runs	VISCOPLEX 10–171 (wt%)	VISCOPLEX 10–312 (wt%)
1	0.7	0.7
2	0.7	1.0
3	1.0	0.7
4	1.0	1.0

laboratory for the preparation of samples having both depressants. The outcomes achieved were then subjected to analysis using the Minitab statistical software. The experimental results were normalized using Eq. 2 considering the fact that the smaller the better is desired in the work, and Eq. 3 was applied to calculate the deviation sequence [31]. Eq. 4 was utilized to determine the grey relational coefficient, which quantifies the relationship between the ideal sequence and the actual experimental data [26]. Furthermore, the grey relation grading was done using the expression in Eq. 5 for the ith experiment [26]. The resulting grey relational grading was subsequently subjected to Taguchi optimization using Minitab and the predicted value was determined using eq. 6 for the validation of analysis.

$$x_i(k) = \frac{max y_i(k) - y_i(k)}{max y_i(k) - min y_i(k)} \tag{2}$$

$x_i(k)$ denotes the normalized value for the ith experiment, $y_i(k)$ represent the initial corresponding analyzed output for each response.

$$\Delta_{oi}(k) = |x_o(k) - x_i(k)| \tag{3}$$

The deviation sequence is denoted by $\Delta_{oi}(k)$, x_o is the the reference value and x_i is the sequence for comparison.

$$\xi_i(k) = \frac{\Delta_{min} + \zeta \Delta_{max}}{\Delta_{oi}(k) + \zeta \Delta_{max}} \tag{4}$$

The grey relational coefficient (GRC) is denoted as $\xi(k)$, Δ_{min} and Δ_{max} are the minimum and maximum deviation of each response variable respectively. ζ is the discriminant coefficient, denoted by $\zeta \in [0,1]$, with a common assignment of 0.5. This assignment promotes moderate discrimination and enhances the overall stability of the results.

$$\gamma_i = \frac{1}{n} \sum_{i=1}^{n} \xi_i(k) \tag{5}$$

γ_i is the grey relational grading and n is the aggregate count of the performance characteristics.

$$\gamma_{predicted} = \gamma_m + \sum_{i=1}^{q} \gamma_o - \gamma_m \tag{6}$$

γ_o is the maximum grey relational grade value obtained for each of the factors in the response table, γ_m is the mean of the GRG, and q corresponds to the number of parameters used.

3. Results and discussion

3.1. Acid value

Monitoring acidity serves as a vital tool for tracking the degradation rate of insulating liquids [47]. The acid level within these liquids can be indicative of their condition. While the oxidation of an insulating liquid typically contributes to increased acidity, primarily due to the oxidation of hydrocarbons, intriguing findings outlined in [14] shed light on an alternate scenario. These results reveal that the rise in the acid content of vegetable-based insulating oil can be attributed to both oxidation and hydrolysis. Notably, this phenomenon could be linked to the presence of glycerides in vegetable oil, compounds known to be susceptible to hydrolysis, as discussed in reference [48]. Fig. 4 depicts the acid values for both fresh samples and those that have undergone aging. Every fresh sample, encompassing the commercially obtained canola oil, the blended oil, and the synthesized methyl ester, aligns with the total acid number established standards outlined by the IEC for new insulating oil [7]. In each case, the total acid number remains below 0.6 mgKOH/g. It's worth noting that liquids containing short-chain fatty acids are considerably more vulnerable to hydrolysis compared to those containing long-chain fatty acids. This is attributed to the steric hindrance effect and larger molecular size exhibited by long-chain fatty acids like C18, which renders them less prone to hydrolysis [49,50]. Furthermore, this phenomenon can be attributed to the hydrophobic nature of fatty acid molecules, which intensifies as the alkyl chain lengthens. The elongation of the chain leads to an increase in molar mass, contributing to enhanced repulsive Van der Waals interactions. These heightened interactions enhance the hydrophobicity of the molecule, making it less susceptible to hydrolysis. Nonetheless, the transesterification process, which involves glycerol removal, results in a decrease in the molecular weight of the liquids and the proportion of polyunsaturated fatty acids [21]. Consequently, this renders the liquid more susceptible to hydrolysis and imparts it with higher oxidation stability, respectively. Hence, considering the conditions previously discussed concerning long-chain and short-chain fatty acids, the increase in acid value observed in sample A, predominantly comprising long-chain fatty acids, could potentially be attributed to oxidation, whereas that seen in sample E could be primarily linked to hydrolysis. Throughout each stage of the oxidation process, the acid value observed in sample A consistently remains lower than that in sample E. This variance might be initiated from a higher production of free fatty acids generated during the hydrolysis of methyl esters, compared to the oxidation reaction in sample A. Furthermore, the oxidation process gives rise to a range of oxidation products, including alcohol, water, aldehyde, and acids. Conversely, the hydrolysis process predominantly yields free fatty acids in their acid form [11].

The composite samples B, C, and D exhibit noticeable differences in behavior within the initial 24-h period, potentially influenced by the presence of saturated fatty acids. This presence seems to slow down the degradation rate of the mixture. As depicted in Fig. 4, the composite liquids display the least acidic values till 24 h of accelerated aging. Nevertheless, a steep rise in acidity becomes evident at the 36-h and 48-
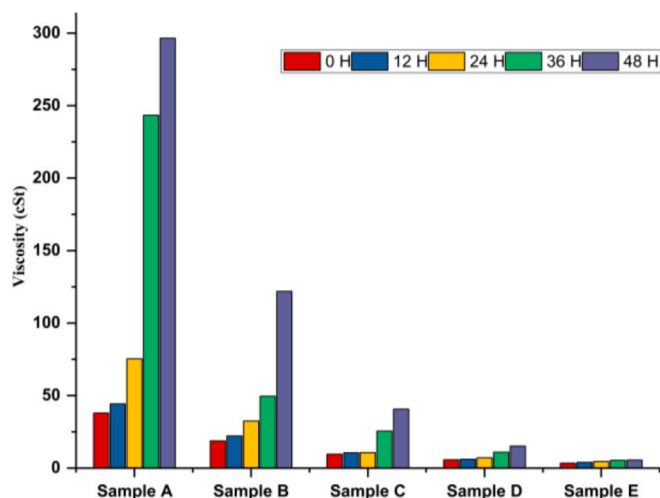

Fig. 4. Total acid number of all the samples from 0 to 48 h.

h marks, likely due to an increased concentration of free fatty acids resulting from the gradual hydrolysis of the saturated (short-chain) fatty acids over time.

3.2. Viscosity

The viscosity of transformer insulating liquids holds significant importance when assessing the transformer's operational lifespan. Throughout the years of operation, oxidation emerges as a notable influencer capable of swiftly elevating the viscosity of such liquids. A rise in the viscosity of the insulating liquid has the potential to impact the cooling system, potentially resulting in overheating and eventual thermal breakdown of the entire system. In order to gain deeper insights and provide clarity regarding the previously mentioned rise in acidity, an assessment of viscosity was carried out on all the samples. Earlier research has firmly established that viscosity escalation is primarily linked to oxidation [51]. In parallel, the increase in acidity can be ascribed to a dual influence, both oxidation and hydrolysis play contributing roles [52–54]. When oil oxidization occurs in insulating liquid, there is a formation of oxygenated functional groups in the by-products which leads to an enhanced Van der Waal interaction. These interactions prevent the molecular planes from sliding over each other, manifesting as increased resistance to flow.

Fig. 5 visually displays the viscosity values of all the samples. Under severe oxidation condition, the intermediate oxidative by-products polymerised to yield high molecular weight substances, which means rise in viscosity. Although there was a noticeable upsurge in viscosity across all samples, the percentage of increase diverged as oxidation time advanced. Specifically, sample A exhibited a substantial percentage escalation in viscosity over time, potentially linked to the oxidation process. Conversely, in the scenario of sample E, the variation in viscosity among samples exposed to different time durations was not pronounced and could be disregarded. This observation effectively validates the notion introduced in the prior section, indicating that the heightened acidity in the case of methyl ester could indeed be attributed to a hydrolysis mechanism. That no sludge is formed during aging means that the fluid possess cooling characteristics similar to unaged oil (almost constant viscosity). Sample B similarly exhibited a notable percentage increase in viscosity. However, a distinct pattern emerged for samples C and D, where significant alterations in viscosity were not evident until the 36-h mark of aging. This phenomenon might be attributed to the proportion of saturated fatty acids present in samples C and D, which seemingly impede the initiation of rapid oxidation reactions within these samples. This is in agreement with the report made in reference [14] where open and sealed beaker thermal aging was considered.

3.3. Fourier transform infrared spectroscopy

Fourier transform analysis was utilized to understand the alterations in the chemical composition of the liquid properties during the aging process. The FTIR spectra of the samples are depicted in Fig. 6. The spectral region ranging from 3000 cm^{-1} to 4000 cm^{-1} was examined to analyze changes in the absorption band area, specifically associated with the stretching vibration of hydroxyl (OH) groups [11,13]. An increase in OH group concentration within an insulating liquid due to aging can lead to heightened absorption band area, as both hydrolysis and oxidation of natural esters yield molecules containing OH groups, such as alcohols and organic acids. The proportional relationship between peak area and concentration is aligned with the principles of the Beer-Lambert law [55]. Fig. 6 (a-e) illustrates a noticeable trend: As aging time progresses, there is a corresponding augmentation in the area beneath the absorption peak.

This observation can be correlated with a gradual rise in the concentration of hydroxyl groups over the duration of aging. The consistent aging pattern exhibited across all samples, spanning from 0 h to 48 h, is in harmony with the acid value outcomes previously mentioned. The spectra of all the samples were compared at every hour of aging and can be seen in Fig. 6 (f-j). In Fig. 6f, depicting the results for all fresh samples, a notable observation emerges: canola oil exhibits the smallest absorption peak area. In contrast, the mixture and pure methyl ester samples showcase heightened areas. This contrast in absorption could potentially be attributed to residual moisture introduced during the water washing step, as detailed in the methodology section. Fig. 6 g and h which are 12 and 24 h of aging time respectively also revealed the thermal stability of samples C and D. Both samples C and D have the least area under the curve and this can be related to low concentration of hydroxyl group at these time intervals. At 36 and 48 h, in Fig. 6 i and j respectively, all the samples assume almost the same pattern exhibiting a disappearing peak previously existing between the range of 3468 to 3474 cm^{-1}.

The rise in the intensity of the carbonyl stretching band around 1740 cm^{-1} serves as a measure to track insulating oil oxidation, indicating the development of carboxylic acids and aldehydes [13]. Monitoring the carboxyl evolution in samples a-e was conducted using ATR-FTIR on a carry 630 spectrometer in transmission mode. As depicted in Figs. 7a-e, the results illustrate that with increased aging duration, the initially narrow peak becomes broader and shifts toward the upper portion of the graph. This spectral alteration is attributed to the growing presence of carboxyl groups due to prolonged oxidation in the presence of oxygen. While all samples exhibited a similar evolution pattern, noteworthy distinctions were observed in samples C and D. Particularly, there was a lack of significant evolution in the C=O peak during the initial 0–24 h for samples C and D, aligning with previous findings detailed in the preceding sections.

3.4. Dielectric spectroscopy

Frequency domain dielectric spectroscopy analysis was employed to gain insights into the behavior of all the samples over the aging time. The importance of this analysis has been explicitly stated in reference [9, 56]. The oxidation of insulating liquid results in the generation of radicals and polymeric impurities. These impurities contribute to elevated values of the dissipation factor within the liquid. Furthermore, as a byproduct of the hydrolysis of natural esters, the resultant acids might dissociate into H$^+$ ions, thereby potentially contributing to a rise in the dissipation factor [6,57]. The rise in dielectric loss is influenced by polarization and conductivity; essentially, both oxidation and hydrolysis lead to an augmentation in the dielectric loss.

Figs. 8a-e exhibit spectra depicting the frequency-dependent dissipation factor behavior across all samples studied. The observed trend indicates an increase in dielectric dissipation factor as aging time progresses, both in pristine samples (A, E) and composite samples (B, C, D). This trend aligns with dielectric theory and is consistent with prior literature findings [12,14,38]. Fig. 8c highlights a notable stability in the dielectric loss of sample C compared to the others at 0, 12, and 24 h. This observation concurs harmoniously with the outcomes of total acid number analysis, viscosity measurements, and FTIR spectroscopy.

Fig. 8 f-j presents a detailed hourly analysis for each sample. Remarkably, at the onset of the aging process (0 h), Sample A exhibited the lowest dielectric loss in comparison to samples containing methyl esters and the methyl ester itself. This could be a result of several steps in methyl ester preparation that might have infused some traces of moisture and probably some traces of ionic impurities in the methyl ester. Moreover, the elimination of glycerol leads to a decrease in the viscosity of the oil, potentially impacting the mobility of charges within the liquid. This phenomenon finds a correlation with Stokes' law, which establishes the interrelationship between charge mobility and the viscosity of dielectric liquids [38]. Nevertheless, with the progression of time from 0 to 24 h of aging, the disparity diminishes, and nearly all samples converge to a similar value, except for sample E. Upon comparing Figs. 8 f-j with the acidity data depicted in Fig. 4, a noticeable correlation emerges: the dielectric loss outcomes align with the observed

(a)

(b)

(c)

(d)

(e)
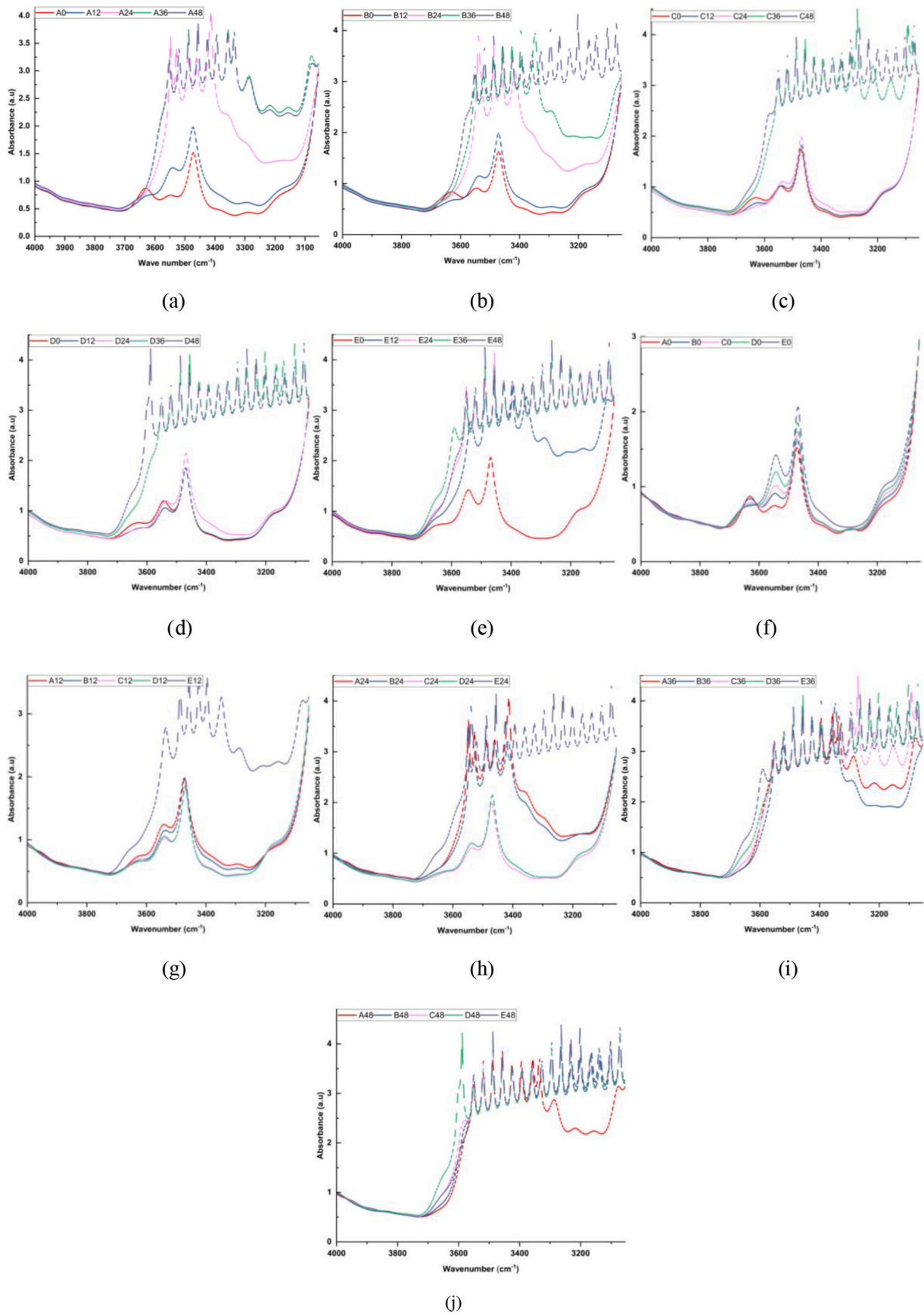

(f)

(g)

(h)

(i)

(j)

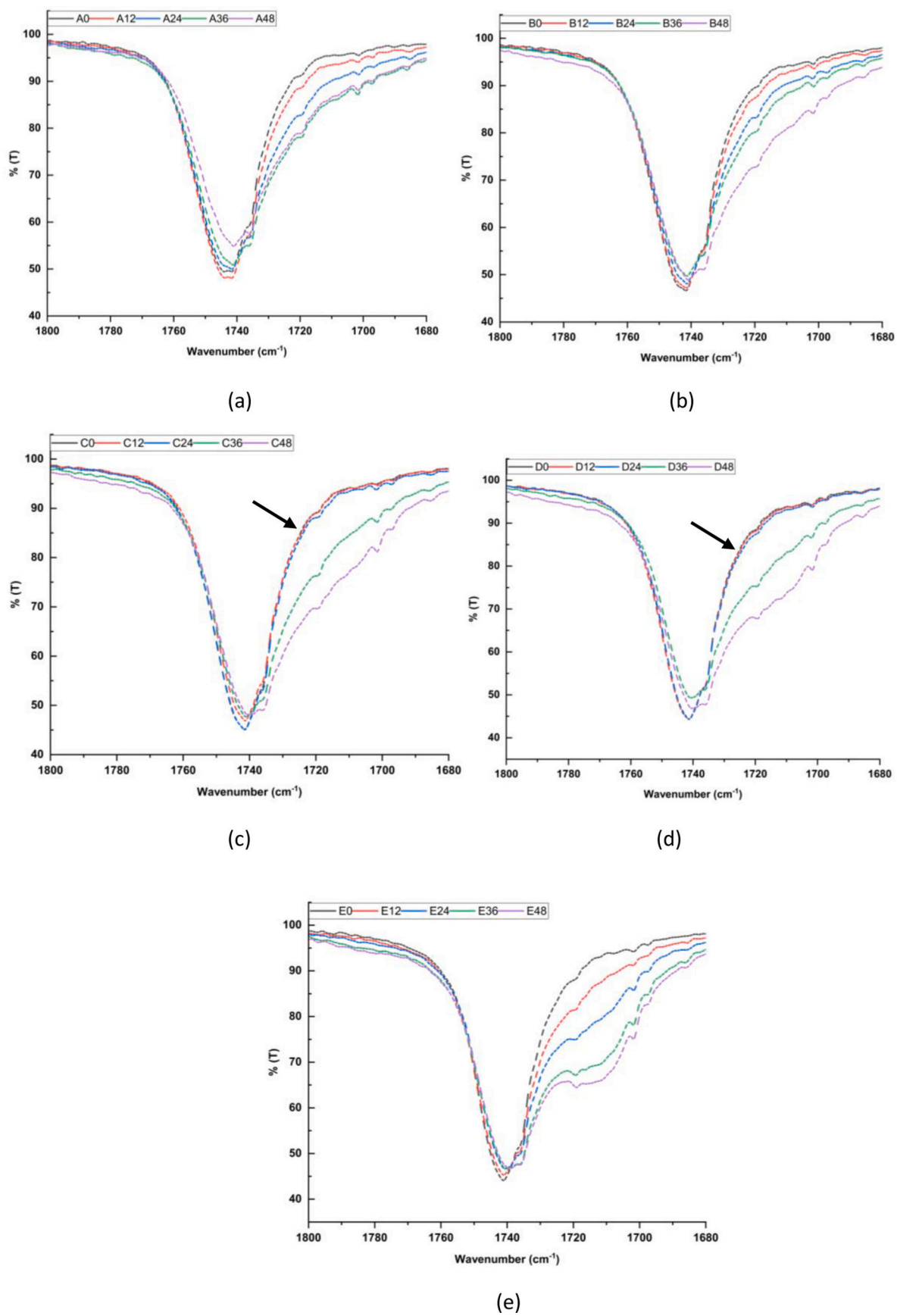**Fig. 5.** Viscosity of all the samples from 0 to 48 h.

Fig. 6. (a-e) FTIR Spectra of fresh samples and their corresponding aged samples, (f-j), the spectra comparing all the samples at every stage of aging.
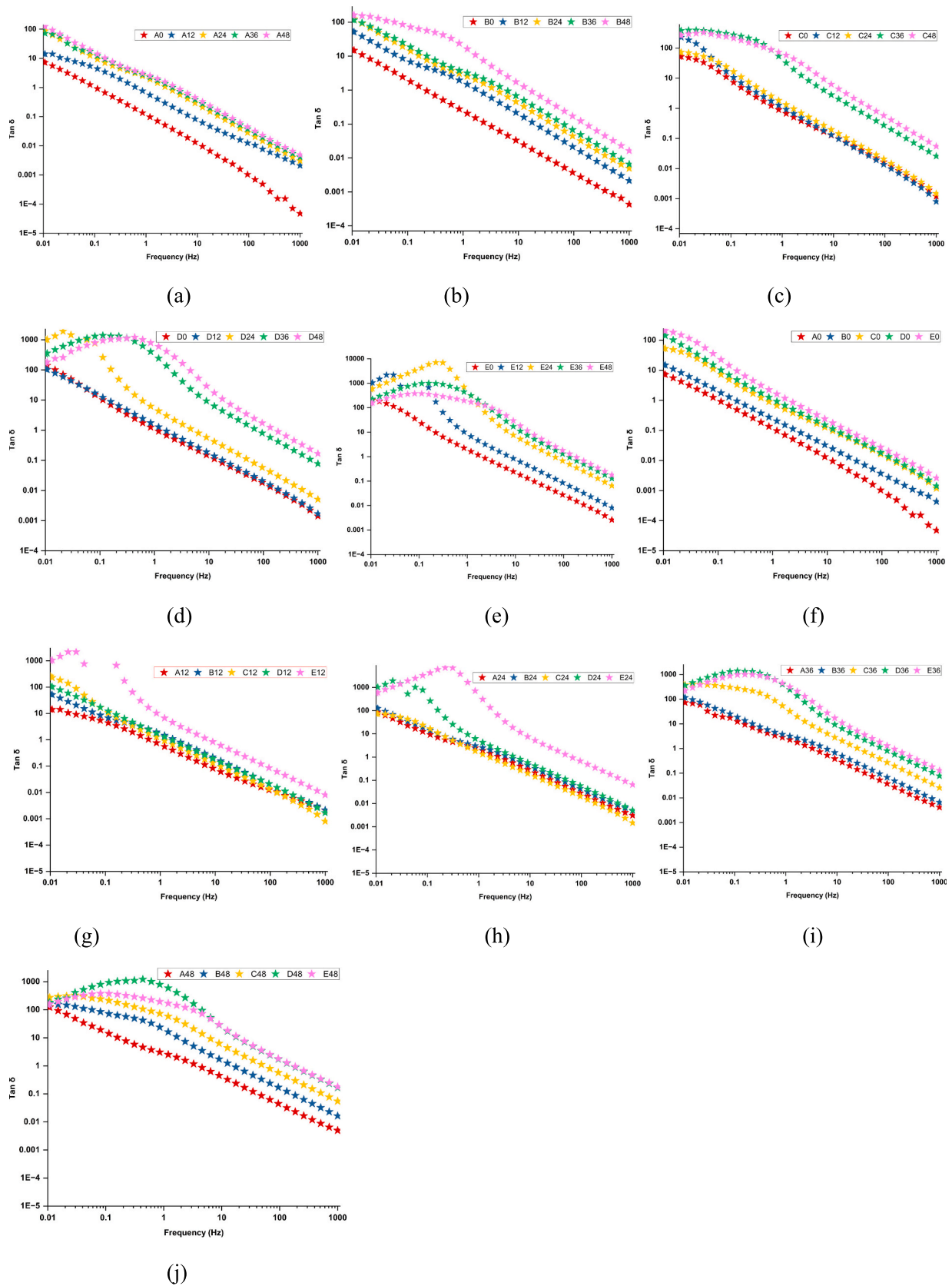
Fig. 7. ATR-FTIR Spectra of fresh samples and their corresponding aged samples.

trend of heightened acidity.

The alignment of all parameters employed in the sample analysis is apparent, establishing them as indicators for comprehending alterations in both the physicochemical and dielectric attributes of aged oil samples. Considering the comprehensive analyses performed on the aged samples, the choice of sample C as the foundational specimen for pour point analysis is substantiated. This decision is rooted in the collective findings elucidated above and is driven by an equilibrium between saturated and unsaturated fatty acids.

Fig. 8: (a-e) Dielectric spectra of fresh samples and their corresponding aged samples, (f-j), Dielectric spectra comparing all the samples at every stage of aging.

3.5. Thermal analysis, Taguchi and Grey computational analysis

The data presented in Table 6 represents the experimental output resulting from the combination of the two pour point depressants. The experimental responses considered are viscosity, acidity, and pour point temperature. The factors considered for the grey relational analysis are viscosity and acidity but the experimental response for the pour point temperature was graphically reported. Pour point temperature was not included in the grey analysis due to its different numerical range, which could lead to a large residual error and potentially affect the accuracy of the analysis. The experimental values for acidity and viscosity were normalized to standardize all variables to a common scale. This process ensures that each factor contributes proportionally and enables a fair comparison by eliminating the impact of absolute values. The normalized data, obtained using eq. 2, is displayed in Table 7. Once the experimental results have been scaled to a range between 0 and 1, the deviation sequence for these two experimental outcomes was computed and displayed in Table 8. The reference point is established as one, serving as a benchmark in relation to the ideal sequence utilized during the normalization process. The grey relational coefficients (GRC) and the grey relational grade (GRG) for each response are calculated using Eq. 4 and 5 respectively, with a distinguishing coefficient of 0.5 for the GRC, and these coefficients are presented in Table 9. The grey relational grade was achieved for the two experimental responses by taking the average of the responses in each experimental run. This helps in turning the two experimental runs into a singular response.

The cooling properties of vegetable oils are significantly influenced by their fundamental composition. Vegetable oils consist of various fatty acids with distinct melting points, resulting in a range of values for both melting and crystallization points rather than a specific temperature [38]. In this study, the behavior of the base sample and the prepared experimental samples was analyzed using a DSC machine, and the results are presented in Table 5. Notably, when two different liquids with differing thermodynamic properties at low temperatures are mixed, their characteristics are retained during cooling. This observation is likely due to variations in their fatty acid compositions.

The onset temperature, representing the temperature at which oil crystallization initiates, and the peak temperature, denoting the highest temperature reached during the crystallization process, were reported to assess the impact of the added depressants. It was evident that the inclusion of depressants had a positive effect on both the onset and peak temperatures, shifting them to lower temperature ranges. From Table 5,

Table 5
Thermal properties of the prepared samples.

Sample	Crystallization temperature (°C)	
	Onset	Peak
00	−12.58	−32.83
1	−13.81	−34.22
2	-13.8	−34.16
3	−13.81	−34.13
4	−14.05	−34.53

Table 6
Experimental results from the two parameters.

Experimental runs	VISCOPLEX 10–171	VISCOPLEX 10–312	Viscosity	Acidity
1	0.7	0.7	13.2	0.055
2	0.7	1.0	13.83	0.111
3	1.0	0.7	13.84	0.128
4	1.0	1.0	14.43	0.129

Table 7
Normalized experimental result taking 1 as the ideal sequence.

Experimental runs	Viscosity	Acidity
1	1	1
2	0.48780	0.24324
3	0.479674	0.01351
4	0	0

Table 8
Deviation sequence.

Experimental runs	Viscosity	Acidity
1	0	0
2	0.5122	0.75676
3	0.520326	0.98649
4	1	1

Table 9
The grey relational coefficient and grey relational grading.

Experimental runs	Viscosity	Acidity	GRG
1	1	1	1
2	0.493	0.397	0.445
3	0.490	0.336	0.413
4	0.333	0.333	0.333

Table 10
GRG Response Table for Means.

Level	VISCOPLEX 10–171	VISCOPLEX 10–312
1	0.7230	0.7066
2	0.3733	0.3896
Delta	0.3497	0.3170
Rank	1	2

Table 11
ANOVA of means for GRG.

Source	Degree of freedom	Adj MS	F	Percentage contribution
VISCOPLEX 10–171	1	0.12228	2.18	43.83%
VISCOPLEX 10–312	1	0.10048	1.79	36.01%
Residual error	1	0.05622		
Total	3	0.27898		

the sample with mark 00 is the sample without depressants which shows an onset temperature at −12.58 °C. The onset temperature at this point could be related to the presence of saturated fatty acids from palm kernel oil. The peak temperature for the sample without depressants was observed at −32. 83 °C which may be attributed to the long unsaturated fatty acids present in the mixture [58]. The table demonstrates that the addition of depressants results in a decrease in temperatures, both for the onset and peak of crystallization. This phenomenon occurs because the depressants, which act as anti-crystallizing agents, effectively delay

the three-dimensional formation of crystals in the liquid [6]. The optimum performance is observed when 1 wt% of both depressants are added. However, it is important to note that while there is a decrease in the crystallization temperature as the depressant concentration increases, it is crucial to consider the overall impact on other parameters to ensure the preservation of the chemical and electrical properties of the base sample. Balancing the desired effect on the low temperature properties without potential changes in other properties is essential to maintain the integrity of the sample. Optimizing the effect of pour point depressants on acidity and viscosity was considered in 3.5.1.

3.6. Taguchi analysis for GRG

The average Grey Relational Grade (GRG) calculated from Table 9 is 0.548111, and the optimal experimental setting is set to 1, corresponding to a 0.7% loading of both depressants. Table 10 ranks the responses based on the analysis of GRG values using the Taguchi methodology, showing the high significance of VISCOPLEX 10–171 as it occupies the first rank, followed by VISCOPLEX 10–312 in the second rank. This implies that VISCOPLEX 10–171 has more impact compared to the other when considering the effect of the pour point depressant on the physicochemical properties of the insulating liquid. The percentage contribution of each parameter was also analyzed from the analysis of variance of means in Table 11. It was further affirmed that VISCOPLEX 10–171 has the highest percentage contribution at 43.83%, compared to VISCOPLEX 10–312 with 36.01%. However, the results show that both depressants have a significant contribution to both the viscosity and acidity values of the insulating liquid. Fig. 9 provides a graphical representation of the Grey Relational Grade from Minitab, presenting a pictogram of the values from the response table.

The predicted value was calculated using Eq. 6 and determined to be 0.8815. The deviation between the predicted and experimental values was calculated using the Root Mean Square Error (RMSE) presented in Eq. 7. The RMSE was computed to be 0.05925, indicating a relatively low level of error and highlighting the close agreement between the predicted and experimental values. It is important to note that larger experimental datasets often yield lower errors and greater accuracy. However, for this study, a smaller dataset was chosen to optimize cost and time efficiency.

Taking all the responses into consideration, the optimum crystalizing temperature when both depressants were used was obtained at a loading of 1% for both depressants. However, for ideal insulating liquids, low acidity and viscosity are required for good insulating conditions and easy circulation, which was observed when 0.7% of both depressants were used. The addition of 0.7% of both depressants slightly increased the acidity from 0.05 mgKOH/g to 0.055 mgKOH/g and the viscosity from 9.6 cSt to 13.2 cSt, showing no significant difference. This finding aligns with the results reported in [2]. This outcome is desirable, as maintaining low acidity and viscosity is essential for the proper health

Fig. 8. Main effect plot for Means (Larger is better).

condition of a transformer. Although 1% loading of both depressants provides the optimum crystallization temperature performance, the effect of the depressants on other factors remains significant. Based on the Grey Relational Grade (GRG) and the experimental results presented in this work, the optimum factor loading to consider when accounting for responses like acidity and viscosity is 0.7% loading.

$$RMSE = \sqrt{\frac{1}{n}\sum \left((Observed\ value - Predicted\ value)^2 \right)} \qquad (7)$$

Where n is 1, the observed value is 1 and the predicted value is 0.8815.

4. Discussion

The degradation caused by oxidation poses a significant challenge for natural esters when utilized in transformers. As outlined in the introduction, this poor oxidation stability is often linked to the composition of fatty acids present in the oil. In this study, two oils with differing properties were examined, leading to their combined use due to their complementary characteristics. Initial assessments revealed that all fresh samples met the required acidity and viscosity standards for new insulating liquids [7,59]. Throughout the oxidation assessment, the properties of all the samples were measured every 12 h and it was observed that samples containing equal volume of both liquids, sample C have the lowest acid value at 24 h relative to commercially available oil, sample A, as shown in Fig. 4. However, subsequent measurements at 36 and 48 h revealed an increase in acidity across all samples, particularly those containing palm kernel methyl ester. The rise in acidity after 24 h may be attributed to the hydrolysis of short-chain fatty acids present in the mixed liquids. This implies that during monitoring of oil-immersed transformers containing a high percentage of saturated fatty acids, an increase in the total acid number of the oil might not imply oil oxidation but hydrolysis of the short-chain fatty acids. The measured viscosity of the oil samples confirmed that the increase in acidity of the mixed oil is due to hydrolysis since no substantial increase in viscosity of the liquids containing a high percentage of methyl ester is observed at every stage of oxidation. From Fig. 5, no significant increment in viscosity was observed for sample C from 0 to 24 h indicating a good oxidation stability of the particular sample. In addition, the percentage increase in viscosity of samples containing methyl ester is lower compared to sample A which implies that the addition of methyl ester reduces the rate of oxidation process in canola base insulting liquid. The absorbance and the transmittance from fitr taken at 3000 cm^{-1} to 4000 cm^{-1} and 1740 cm^{-1} were used to monitor the variation in the hydroxyl and carbonyl generation of the samples respectively. It was observed in Fig. 6 that as the oil aged, the absorption band area increased which could be attributed to the stretching vibration of the hydroxyl group generated during the aging process of the oil by oxidation. Similarly, the development of carboxylic acids and aldehydes was monitored at 1740 cm^{-1} in Fig. 7 and it was observed that as the liquids aged, the peak of the samples became broader. In Fig. 7c and d no observable changes in the spectra at 0 to 24 h which implies that samples C and D are relatively stable to oxidation, consistent with the acidity and viscosity results.

Dielectric loss spectra (Fig. 8 a-e) demonstrated an increase with aging time, attributed to the generation of oxidation by-products, which elevate loss and conductivity. However, in Fig. 8c, the sample containing 50% of canola oil and 50% of palm kernel oil methyl ester, no significant changes were observed in the dielectric loss over 24 h of the oxidation process. The dielectric loss stability can be considered to be proportional to the oxidation stability of the liquid which has been previously investigated. Moreover, in Fig. 8 h, among all the samples, sample C shows the lowest dielectric loss, an indication of higher oxidation stability. It is to be mentioned that the increase in dielectric loss at 36 and 48 h for samples containing methyl ester is due to an increased acid value due to hydrolysis as previously mentioned. Sample C, identified as
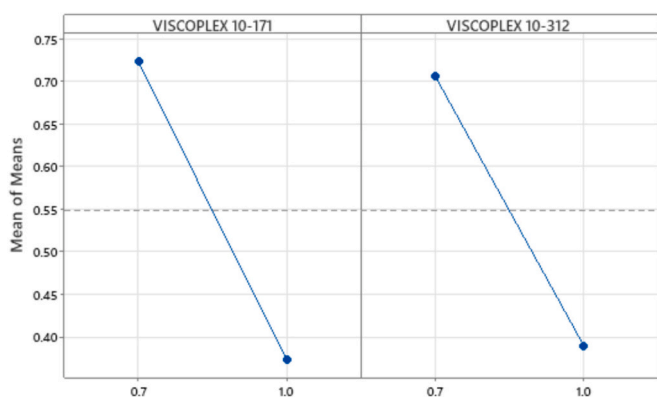
the most stable to oxidation, was chosen for cold flow enhancement. The addition of flow improvers was found to reduce both the onset and peak temperatures, with an optimal loading of 1 wt%. These additives prevent crystallization, thereby enhancing flow properties in low temperatures. Analysis using Taguchi-grey relational analysis revealed that a 0.7 wt% loading of flow improvers significantly enhanced properties without altering the base liquid properties significantly. This assessment suggests that a liquid mixture comprising equal volumes of canola oil and methyl ester, supplemented with 0.7 wt% of both flow improvers, could effectively serve as an insulating liquid in low-temperature regions while maintaining good thermal stability.

5. Conclusion

The experimental and statistical techniques applied in this study to enhance oxidation stability and crystallization temperature have generated several significant insights and observations, which can be summarized as follows:

i. The mixture of canola oil and palm kernel oil methyl ester in an equal ratio exhibits superior stability to oxidation, as evidenced by results, particularly from Fourier Transform Infrared Spectroscopy (FTIR). The noticeable increase in acidity of the sample with an equal proportion of oils after 24 h of oxidation indicates hydrolysis of the short fatty acids in the mixture, rather than an oxidation process, as the percentage rise in viscosity is negligible. The marginal increase observed in the viscosity of oxidized oils may be attributed to the presence of oxygenated functional groups in the byproduct, enhancing Van der Waals interactions and impeding molecular planes' sliding over each other. To address hydrolysis in the sample with an equal ratio of oils and achieve oil with reduced acidity, exploring side chain branching of the mixture or precise addition of antioxidants to the base oil could be beneficial. While the generated acidity (free fatty acid) is generally considered harmless to transformer components, minimizing acidity is crucial to prevent high conductivity in the insulating liquid.

ii. Optimization of the pour point depressants effect conducted through Taguchi-grey relational analysis provides crucial insights. It is concluded that the addition of both VISCOPLEX 10–171 and VIS-COPLEX 10–312 to the base samples has a positive impact on enhancing the crystallization temperature of the insulating liquid in cold climate regions without significantly complicating other physicochemical properties. Furthermore, the environmental friendliness of the synthesized liquid remains uncompromised, as the pour point depressants added are entirely eco-friendly and biodegradable.

The significance of the oil synthesized in this study cannot be overstated, as it emerges as a notable substitute for mineral-based insulating liquids. The widespread acceptance of natural insulating liquids not only minimizes environmental impact but also advances sustainable agricultural practices thereby reducing global warming. Therefore, this work suggests the need for further study involving a larger experimental dataset to enhance optimization accuracy. Additionally, investigating the impact of depressants on the base liquid under high electric fields is essential. Moreover, investigating the impact of multiple antioxidants on the base sample carries substantial importance for both the academic and industrial sectors.

CRediT authorship contribution statement

S.O. Oparanti: Writing – original draft, Visualization, Validation, Methodology, Investigation, Funding acquisition, Formal analysis, Conceptualization. **I. Fofana:** Funding acquisition, Resources, Supervision, Validation, Writing – review & editing. **R. Zarrougui:** Validation, Writing – review & editing. **R. Jafari:** Validation, Writing – review & editing. **K.M.L. Yapi:** Investigation, Visualization.

Declaration of competing interest

The authors declare no known competing financial interests or personal relationships.

Data availability

Data will be made available on request.

Acknowledgments

References

[1] D.K. Mahanta, Green transformer oil: A review, in: in 2020 IEEE International Conference on Environment and Electrical Engineering and 2020 IEEE Industrial and Commercial Power Systems Europe (EEEIC/I&CPS Europe), IEEE, Madrid, Spain, 2020, pp. 1–6, https://doi.org/10.1109/EEEIC/ICPSEurope49358.2020.9160654.

[2] T. Yang, et al., Low-temperature property improvement on green and low-carbon natural ester insulating oil, IEEE Trans. Dielectr. Electr. Insul. 29 (4) (2022) 1459–1464.

[3] C. Perrier, T. Stirl, Moisture-equilibrium charts: monitoring natural-ester green transformers, Transformers Magazine 4 (2) (2017) 98–102.

[4] G. Power, Transformers, Inside Housing (2002) 16–17.

[5] Z.B. Siddique, S. Basu, P. Basak, Dielectric behavior of natural ester based mineral oil blend dispersed with TiO2 and ZnO nanoparticles as insulating fluid for transformers, J. Mol. Liq. 339 (2021) 116825.

[6] S.O. Oparanti, U.M. Rao, I. Fofana, Natural esters for green transformers: challenges and keys for improved serviceability, Energies 16 (1) (2023) 61, https://doi.org/10.3390/en16010061.

[7] D.M. Mehta, P. Kundu, A. Chowdhury, V. Lakhiani, A. Jhala, A review on critical evaluation of natural ester Vis-a-vis mineral oil insulating liquid for use in transformers: part 1, IEEE Trans. Dielectr. Electr. Insul. 23 (2) (2016) 873–880.

[8] F. Wang, et al., Enhancing Dielectric and Thermal Performances of Synthetic-Ester Insulating Oil via Blending With Natural Ester, in: in IEEE Transactions on Dielectrics and Electrical Insulation, 30 (3), 2023, pp. 1115–1125, https://doi.org/10.1109/TDEI.2023.3243158.

[9] U.M. Rao, I. Fofana, R. Sarathi, Alternative Liquid Dielectrics for High Voltage Transformer Insulation Systems: Performance Analysis and Applications, John Wiley & Sons, 2021.

[10] H. Cong, H. Shao, Y. Du, X. Hu, W. Zhao, Q. Li, Influence of nanoparticles on long-term thermal stability of vegetable insulating oil, IEEE Trans. Dielectr. Electr. Insul. 29 (5) (2022) 1642–1650, https://doi.org/10.1109/TDEI.2022.3190805.

[11] K. Bandara, C. Ekanayake, T.K. Saha, P.K. Annamalai, Understanding the ageing aspects of natural ester based insulation liquid in power transformer, IEEE Trans. Dielectr. Electr. Insul. 23 (1) (2016) 246–257.

[12] C.M. Gutiérrez, C.O. Salmas, C.J.R. Estébanez, M. Kozako, M. Hikita, A. O. Fernández, Study of the Thermal Degradation of Different Insulating Papers Impregnated with a Natural Ester, in: in 2022 9th International Conference on Condition Monitoring and Diagnosis (CMD), IEEE, 2022, pp. 167–171.

[13] U.M. Rao, I. Fofana, P. Rozga, P. Picher, D.K. Sarkar, R. Karthikeyan, Influence of gelling in natural esters under open beaker accelerated thermal aging, IEEE Trans. Dielectr. Electr. Insul. 30 (1) (2022) 413–420.

[14] Y. Xu, S. Qian, Q. Liu, Z. Wang, Oxidation stability assessment of a vegetable transformer oil under thermal aging, IEEE Trans. Dielectr. Electr. Insul. 21 (2) (2014) 683–692.

[15] S. Ab Ghani, N.A. Muhamad, Z.A. Noorden, H. Zainuddin, N.A. Bakar, M.A. Talib, Methods for improving the workability of natural ester insulating oils in power transformer applications: a review, Electr. Power Syst. Res. 163 (2018) 655–667.

[16] M. Hamid, M. Ishak, M.M. Din, N. Suhaimi, N. Katim, Dielectric properties of natural ester oils used for transformer application under temperature variation, in: 2016 IEEE International Conference on Power and Energy (PECon), IEEE, 2016, pp. 54–57.

[17] J.K. Daun, M.N. Eskin, D. Hickling, Canola: Chemistry, Production, Processing, and Utilization, Elsevier, 2015.

[18] K. Murthy, V.M. Kotebavi, Study on performance and emission characteristics of CI engine fueled with canola oil-diesel blends, in: AIP Conference Proceedings vol. 2200, no. 1, AIP Publishing, 2019.

[19] C. Loganes, S. Ballali, C. Minto, Main properties of canola oil components: a descriptive review of current knowledge, The Open Agriculture Journal 10 (1) (2016).

[20] N. Dian, et al., Palm oil and palm kernel oil: versatile ingredients for food applications, Journal of Oil Palm Research 29 (4) (2017) 487–511.

[21] S.O. Oparanti, A.A. Adekunle, V.E. Oteikwu, A.I. Galadima, A.A. Abdelmalik, An experimental investigation on composite methyl ester as a solution to environmental threat caused by mineral oil in transformer insulation, Biomass Convers. Biorefinery (2022) 1–11, https://doi.org/10.1007/s13399-022-03286-3.

[22] C. Jin, et al., Preparation and performance improvement of methanol and palm oil/palm kernel oil blended fuel, Fuel Process. Technol. 223 (2021) 106996.

[23] A. Ayoola, et al., Response surface methodology and artificial neural network analysis of crude palm kernel oil biodiesel production, Chemical Data Collections 28 (2020) 100478.

[24] E.O. Oke, et al., Process design, techno-economic modelling, and uncertainty analysis of biodiesel production from palm kernel oil, Bioenergy Res. 15 (2) (2022) 1355–1369.

[25] M.J.H. Akanda, M.Z.I. Sarker, S. Ferdosh, M.Y.A. Manap, N.N.N. Ab Rahman, M. O. Ab Kadir, Applications of supercritical fluid extraction (SFE) of palm oil and oil from natural sources, Molecules 17 (2) (2012) 1764–1794.

[26] J.K. Abifarin, Taguchi grey relational analysis on the mechanical properties of natural hydroxyapatite: effect of sintering parameters, Int. J. Adv. Manuf. Technol. 117 (1–2) (2021) 49–57.

[27] K. Yousefi, H. Daneshmanesh, Optimization of physical and mechanical properties of calcium silicate nanocomposite by Taguchi method, J. New Mater. 11 (39) (2020) 77–90.

[28] S. Javed, A Novel Research on Grey Incidence Analysis Models and its Application in Project Management, Nanjing University of Aeronautics and Astronautics, Nanjing, PR China, 2019.

[29] J.K. Abifarin, D.O. Olubiyi, E.T. Dauda, E.O. Oyedeji, Taguchi grey relational optimization of the multi-mechanical characteristics of kaolin reinforced hydroxyapatite: effect of fabrication parameters, International Journal of Grey Systems 1 (2) (2021) 20–32.

[30] E.J. Kadim, Z.A. Noorden, Z. Adzis, N. Azis, N.A. Mohamad, Surfactants Effects on Enhancing Electrical Performance of Nanoparticle-Based Mineral Transformer Oil, in: in IEEE Transactions on Dielectrics and Electrical Insulation, 30 (4), 2023, https://doi.org/10.1109/TDEI.2023.3282910.

[31] S. Senthilkumar, et al., Optimization of transformer oil blended with natural ester oils using Taguchi-based grey relational analysis, Fuel 288 (2021) 119629.

[32] J.K. Abifarin, F.B. Abifarin, E.O. Oyedeji, C. Prakash, S.A. Zahedi, Computational analysis on mechanostructural properties of hydroxyapatite–alumina–titanium nanocomposite, J. Korean Ceram. Soc. (2023) 1–9.

[33] M.E. Arce, Á. Saavedra, J.L. Míguez, E. Granada, The use of grey-based methods in multi-criteria decision analysis for the evaluation of sustainable energy systems: a review, Renew. Sust. Energ. Rev. 47 (2015) 924–932.

[34] A. Agenbag, Canola production and utilisation: an overview, Oilseeds Focus 1 (1) (2015) 6–7.

[35] E.F. Aransiola, M.O. Daramola, T.V. Ojumu, M.O. Aremu, S. Kolawole Layokun, B. O. Solomon, Nigerian Jatropha curcas oil seeds: prospect for biodiesel production in Nigeria, International Journal of Renewable Energy Research 2 (2) (2012) 317–325.

[36] C. Martín, A. Moure, G. Martín, E. Carrillo, H. Domínguez, J.C. Parajó, Fractional characterisation of jatropha, neem, moringa, trisperma, castor and candlenut seeds as potential feedstocks for biodiesel production in Cuba, Biomass Bioenergy 34 (4) (2010) 533–538.

[37] S.O. Oparanti, K.M.L. Yapi, I. Fofana, U.M. Rao, Preliminary studies on Improving the Properties of Canola Oil by Addition of Methyl Ester from a Saturated Vegetable Oil, in: 2023 IEEE Electrical Insulation Conference (EIC), IEEE, 2023, pp. 1–4.

[38] A.A. Abdelmalik, The Feasibility of Using a Vegetable Oil-Based Fluid as Electrical Insulating Oil, University of Leicester, 2012.

[39] S.X. Tan, S. Lim, H.C. Ong, Y.L. Pang, State of the art review on development of ultrasound-assisted catalytic transesterification process for biodiesel production, Fuel 235 (2019) 886–907.

[40] J.L. Jiosseu, A. Jean-Bernard, G. Mengata Mengounou, E. Tchamdjio Nkouetcha, A. Moukengue Imano, Statistical analysis of the impact of FeO3 and ZnO nanoparticles on the physicochemical and dielectric performance of monoester-based nanofluids, Sci. Rep. 13 (1) (2023) 12328, https://doi.org/10.1038/s41598-023-39512-9.

[41] M. Berrios, J. Siles, M. Martin, A. Martin, A kinetic study of the esterification of free fatty acids (FFA) in sunflower oil, Fuel 86 (15) (2007) 2383–2388.

[42] R. Bhoi, D. Singh, S. Mahajani, Investigation of mass transfer limitations in simultaneous esterification and transesterification of triglycerides using a heterogeneous catalyst, React. Chem. Eng. 2 (5) (2017) 740–753.

[43] J.M. Evangelista Jr., F.E.B. Coelho, J.A. Carvalho, E.M. Araújo, T.L. Miranda, A. Salum, Development of a new bio-based insulating fluid from Jatropha curcas oil for power transformers, Advances in Chemical Engineering and Science 7 (02) (2017) 235.

[44] M.H. Roslan, N.A. Mohamad, T.Y. Von, H.M. Zadeh, C. Gomes, Latest developments of palm oil as a sustainable transformer fluid: a green alternative to mineral oils, Biointerface Res. Appl. Chem 11 (5) (2021) 13715–13728.

[45] D. ASTM, 2440, Oxidation Stability of Mineral Insulating Oil, ASTM International, 2004.

[46] A. International, D445-18 standard test method for kinematic viscosity of transparent and opaque liquids (and calculation of dynamic viscosity), Annu. Book ASTM Stand. 1 (2010) 1–10.

[47] C.M. Gutiérrez, A.O. Fernández, C.J.R. Estébanez, C.O. Salas, R. Maina, Understanding the ageing performance of alternative dielectric fluids, IEEE Access 11 (2023) 9656–9671.

[48] M. Amanullah, S.M. Islam, S. Chami, G. Ienco, Evaluation of several techniques and additives to de-moisturise vegetable oils and bench mark the moisture content level of vegetable oil-based dielectric fluids, in: 2008 IEEE International Conference on Dielectric Liquids, IEEE, 2008, pp. 1–4.

[49] Y. Liu, E. Lotero, J.G. Goodwin Jr., Effect of carbon chain length on esterification of carboxylic acids with methanol using acid catalysis, J. Catal. 243 (2) (2006) 221–228.

[50] N.A. Raof, R. Yunus, U. Rashid, N. Azis, Z. Yaakub, Effect of molecular structure on oxidative degradation of ester based transformer oil, Tribol. Int. 140 (2019) 105852.

[51] H. Wilhelm, G. Stocco, S. Batista, Reclaiming of in-service natural ester-based insulating fluids, IEEE Trans. Dielectr. Electr. Insul. 20 (1) (2013) 128–134.

[52] X. Li, et al., Breakdown characteristic of natural ester gelling process under oxidation and its impact on fresh oil, in: 2017 IEEE 19th International Conference on Dielectric Liquids (ICDL), IEEE, 2017, pp. 1–4.

[53] J. Viertel, K. Ohlsson, S. Singha, Thermal aging and degradation of thin films of natural ester dielectric liquids, in: 2011 IEEE International Conference on Dielectric Liquids, IEEE, 2011, pp. 1–4.

[54] U.M. Rao, I. Fofana, Monitoring the Sol and Gel in Natural Esters under Open Beaker Thermal Aging, in: 2021 IEEE 5th International Conference on Condition Assessment Techniques in Electrical Systems (CATCON), IEEE, 2021, pp. 127–131.

[55] J. Gordon, S. Harman, A graduated cylinder colorimeter: an investigation of path length and the beer-Lambert law, J. Chem. Educ. 79 (5) (2002) 611.

[56] N. Chalashkanov, L. Dissado, Dielectric measurements in the frequency domain—dos and Don'ts, IEEE Electr. Insul. Mag. 38 (5) (2022) 28–38.

[57] T. Kano, T. Suzuki, R. Oba, A. Kanetani, H. Koide, Study on the oxidative stability of palm fatty acid ester (PFAE) as an insulating oil for transformers, in: 2012 IEEE International symposium on electrical insulation, IEEE, 2012, pp. 22–25.

[58] I. Foubert, K. Dewettinck, D. Van de Walle, A. Dijkstra, P. Quinn, Physical properties: structural and physical characteristics, The lipid handbook 8 (2007) 535–590.

[59] D.M. Mehta, P. Kundu, A. Chowdhury, V. Lakhiani, A. Jhala, A review of critical evaluation of natural ester Vis-a-vis mineral oil insulating liquid for use in transformers: part II, IEEE Trans. Dielectr. Electr. Insul. 23 (3) (2016) 1705–1712.